

# Synthesis of Thermochemical Iron(II) Tris(bipyridine)-Centered Star-Shaped Polyoxazolines and Their Bipyridine-Centered Macroligand Counterparts

John E. McAlvin, Sarah B. Scott, and Cassandra L. Fraser\*

Department of Chemistry, University of Virginia, McCormick Road, P.O. Box 400319, Charlottesville, Virginia 22904-4319

Received January 7, 2000; Revised Manuscript Received July 11, 2000

**ABSTRACT:** Iron tris(bipyridine) complexes  $[\text{Fe}\{4,4'\text{-bis(chloromethyl)-2,2'-bipyridine}\}_3]$ , **1a**, and the corresponding iodide analogue generated in situ using NaI, **1b**, were explored as initiators for the polymerization of a series of 2-R-2-oxazoline monomers (R = ethyl, EtOX; methyl, MeOX; phenyl, PhOX; and undecyl, UnOX). The resulting labile core, red-violet Fe-centered star polymers fragment during molecular weight analysis by gel permeation chromatography (GPC). Thus, samples were subjected to chemical cleavage in aqueous  $\text{K}_2\text{CO}_3$  to generate metal-free bipyridine-centered polyoxazolines, bpyPROX<sub>2</sub>. When combined with ferrous ammonium sulfate, these bpyPROX<sub>2</sub> macroligands chelate to Fe(II), regenerating the  $[\text{Fe}(\text{bipyridine})_3]^{2+}$  chromophores. Both preparative and analytical kinetics experiments generally produce polymers with reasonably narrow molecular weight distributions ( $\sim 1.1\text{--}1.5$ ). Molecular weight vs % monomer conversion plots with either the iodide or chloride initiating system were nearly linear for all monomers; however, only PEOX and PUOX products show good correlation with  $M_n(\text{calcd})$  based on monomer/initiator loading. For most monomers, reactions with iodide initiators are faster than the chlorides, and linear first-order kinetics plots were observed. Polymerization of oxazolines with 4,4'-bis(halomethyl)-2,2'-bipyridines produced polymers with very narrow molecular weight distributions but with molecular weights higher than targeted based on monomer loading.  $^1\text{H}$  NMR data illustrates that termination with dipropylamine is efficient for EtOX polymerizations. Thermal analysis by DSC and TGA reveal few differences between Fe-centered stars and their bpy-centered PROX macroligand counterparts. Variable-temperature UV/vis data is provided for an Fe-centered PEOX thin film sample.

## Introduction

Iron-containing polymers serve as responsive materials in both natural and synthetic contexts.<sup>1–3</sup> Heme proteins are noted for their oxygen binding ability<sup>4</sup> and for playing important roles in metabolic and electron-transfer pathways.<sup>5,6</sup> Efforts have been made to mimic the biological reactivity of iron complexes with oxygen in model systems.<sup>7–10</sup> And for electron-transfer studies, ferrocene-containing polymers are numerous.<sup>11–13</sup> Iron centers are also frequently utilized as templates in supramolecular and dendrimer chemistry,<sup>14</sup> and often these systems exhibit multiple reversible redox transformations. Metal-containing polymers that fragment in response to light<sup>15,16</sup> or display heat-sensitive ligand dissociation<sup>17</sup> have also been reported.

Previously, we described the preparation of Fe tris(bipyridine)-centered star-shaped polymers (Figure 1) based on poly(2-R-2-oxazoline), PROX (R = ethyl), by a divergent strategy that utilizes hexafunctional  $[\text{Fe}\{\text{bpy}(\text{CH}_2\text{X})_2\}_3](\text{PF}_6)_2$  reagents **1a** and **1b** as the initiators (Figure 2).<sup>18–20</sup> Ruthenium tris(bpy) reagents with different numbers of functional groups were used in the production of luminescent, linear, and star-shaped polymers by a similar approach.<sup>21,22</sup> Schubert and Nuyken have extended this concept by preparing analogous polyoxazolines from related metal bipyridine initiating systems.<sup>23–25</sup> As was noted by Chujo et al. for polyoxazoline hydrogels with numerous metal cross-links,<sup>17</sup> metal PROX materials with a single metal coordination site also respond in interesting ways to chemical, mechanical, thermal, and electrochemical perturbations.

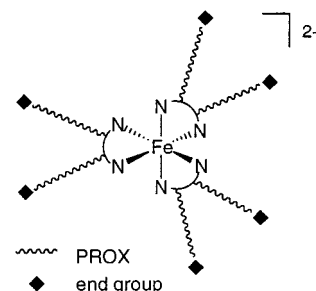


**Figure 1.** Schematic representation of Fe tris(bipyridine)-centered six arm star-shaped polyoxazolines, PROX. End group = oxazolinium cation, alkyl halide, or, after termination,  $-\text{NPr}_2$ .

Polyoxazolines have found application in a variety of contexts<sup>26</sup> as adhesives, surfactants, hydrogels, and ceramic binders and in drug delivery systems.<sup>27</sup> Some of these uses could benefit from the molecular weight and architectural control that may be achieved through living polymerization. By varying the substituent in 2-R-2-oxazoline monomers, it is possible to obtain materials with very different properties, ranging from glassy, water-soluble ethyl and methyl derivatives to crystalline hydrophobic ones with long aliphatic chains.<sup>26</sup> It was of interest to us to couple this ready control over polymer properties with the responsive features that metals introduce. This has been exploited in the preparation of iron-centered star block copolymers<sup>20</sup> that undergo microphase separation in thin and bulk films.<sup>28</sup> In this study, we explore the compatibility of the iron metal-ligand initiators **1a** and **1b** with different 2-R-2-oxazoline monomers (R = ethyl, methyl, phenyl, and undecyl) (Figure 2) under various reaction conditions. Kinetics

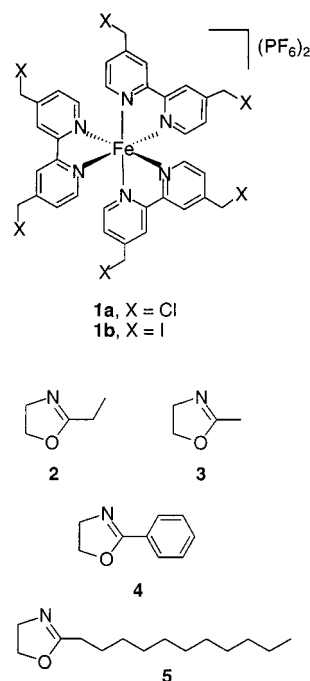


**Figure 2.** Hexafunctional iron initiators,  $[\text{Fe}\{\text{bpy}(\text{CH}_2\text{X})_2\}_3](\text{PF}_6)_2$ , **1a** and **1b**, and oxazoline monomers, EtOX, MeOX, PhOX, and UnOX, **2–5**.

experiments probe the molecular weight ranges over which polymerizations are controlled. Reactions with ligand initiators, 4,4'-bis(halomethyl)-2,2'-bipyridines, with the ethyl monomer are also described. In addition, thermal properties of  $[\text{Fe}(\text{bpyPEOX}_2)_3]^{2+}$  films, including variable-temperature UV/vis spectral analysis, were performed to better understand the thermochromism exhibited by iron tris(bipyridine)-containing polymers.

## Experimental Section

**General Considerations. Materials.** 2-Ethyl-2-oxazoline, 2-methyl-2-oxazoline, 2-phenyl-2-oxazoline,  $\text{CH}_3\text{CN}$ , and  $\text{CD}_3\text{CN}$  were distilled from  $\text{CaH}_2$  prior to use. 1,3-Dioxane was fractionally distilled over sodium prior to use.<sup>29</sup> 2-Undecyl-2-oxazoline was prepared and purified by the method of Jung et al.<sup>30</sup> The ligand, 4,4'-bis(chloromethyl)-2,2'-bipyridine, was prepared as previously described.<sup>31</sup> All other reagents and solvents were used as received unless otherwise indicated.

**Instrumentation.**  $^1\text{H}$  NMR spectra were acquired on a GE QE 300 MHz spectrometer. The molecular weights of polyoxazoline samples, PROX (R = E, ethyl; P, phenyl; U, undecyl) were determined by GPC in  $\text{CHCl}_3$  solution using Polymer Labs 5 $\mu$  Mixed-C columns coupled with Wyatt Technology multiangle laser light scattering (MALLS) and refractive index (RI) detectors and Hewlett-Packard instrumentation and software, as previously reported.<sup>19</sup> Refractive index increments ( $dn/dc$  values) were measured as previously described ( $\text{CHCl}_3$ ,  $\lambda = 633$  nm,  $T = 40$  °C,  $dn/dc$  of  $\text{bpyPEOX}_2 = 0.079$  mL/g,  $dn/dc$  of  $\text{bpyPPOX}_2 = 0.146$  mL/g,  $dn/dc$  of  $\text{bpyPUOX}_2 = 0.059$  mL/g). GPC of PMOX samples (M = methyl) was performed using Polymer Labs 5 $\mu$  Mixed-C columns (2) and a guard column with DMF containing 0.4% triethylamine as the mobile phase. Molecular weights were obtained relative to poly(methyl methacrylate) (PMMA) standards. With the exception of PPOX, thermal analyses of all PROX samples were performed using a TA Instruments DSC 2920 modulated differential scanning calorimeter and a TGA 2020 thermogravimetric analyzer and previously reported methods.<sup>20</sup> For PPOX, DSC measurements were carried out using the following experimental parameters: modulated mode under  $\text{N}_2$ ; amplitude 1 °C; period = 60 s; heating and cooling rate = 5 °C/min. Protocol: heat to 250 °C; cool to 40 °C; heat to 300 °C; cool to

40 °C; heat to 300 °C. Electronic absorption spectra were recorded using a Hewlett-Packard 8453 UV/vis spectrophotometer with UV/vis Chemstation Rev.A.02.05 software. A Harrick HTC-100 high-temperature cell and a Harrick ATC-30D automatic temperature controller were utilized for variable-temperature UV/vis spectral analysis of Fe PROX films.

**$[\text{Fe}\{\text{bpy}(\text{CH}_2\text{Cl})_2\}_3](\text{PF}_6)_2$ , **1a**.** The iron chloride initiator, **1a**, was prepared by the method described by Gould et al. for a similar complex.<sup>32</sup> To a solution of  $\text{Fe}(\text{NH}_4)_2(\text{SO}_4)_2 \cdot 6\text{H}_2\text{O}$  (0.564 g; 1.44 mmol) in MeOH (225 mL) was added 4,4'-bis(chloromethyl)-2,2'-bipyridine (1.13 g; 4.46 mmol). The colorless solution immediately turned dark red. The reaction mixture was stirred at room temperature under a slow stream of  $\text{N}_2$  for 3 h before  $\text{NH}_4\text{PF}_6$  (2.81 g; 17.3 mmol) was added to precipitate a red solid. The suspension was stirred at room temperature for 30 min, collected by filtration, washed with water ( $2 \times 5$  mL), MeOH ( $2 \times 5$  mL), and diethyl ether ( $2 \times 10$  mL) and then was dried in vacuo. Yield: 1.46 g; 92%.  $^1\text{H}$  NMR (300 MHz,  $\text{CD}_3\text{CN}$ ):  $\delta$  4.81 (s, 12H), 7.35 (d,  $J = 6$  Hz, 6 H), 7.43 (d,  $J = 6$  Hz, 6 H), 8.57 (s, 6H).  $^{13}\text{C}$  NMR (75 MHz,  $\text{CD}_3\text{CN}$ ):  $\delta$  44.5, 124.9, 128.2, 151.3, 155.9, 160.5. Anal. Calcd for  $\text{FeC}_{36}\text{H}_{30}\text{N}_6\text{Cl}_6\text{P}_2\text{F}_{12}$ : C, 39.12; H, 2.74; N, 7.60. Found: C, 38.60; H, 2.80; N, 7.50. UV/vis ( $\text{CH}_3\text{CN}$ )  $\lambda_{\text{max}}$ , nm ( $\epsilon$ ,  $\text{M}^{-1}\text{cm}^{-1}$ ): 302 (64 100), 363 (8900), 532 (10 400).

**$[\text{Fe}(\text{bpyPEOX}_2)_3]^{2+}$ , **6**.** Polymerization of EtOX by the iodide initiator **1b**, was performed as previously described.<sup>19</sup> A representative reaction of EtOX with **1a** is as follows: The initiator **1a** (18.0 mg; 0.0163 mmol),  $\text{CH}_3\text{CN}$  (3.30 mL) and EtOX (0.969 g; 9.77 mmol) were added to a Schlenk flask. The mixture was sealed under  $\text{N}_2$  and stirred at 85 °C for 1 d and then was cooled to room temperature for addition of dipropylamine (39.6 mg; 0.391 mmol). The mixture was stirred at room temperature for 15 h and concentrated in vacuo to produce a red solid. The crude product was redissolved in  $\text{CH}_2\text{Cl}_2$  (3 mL) and delivered to stirring  $\text{Et}_2\text{O}$  (35 mL) to precipitate a red glassy polymer. Yield: 0.980 g; 98%.  $^1\text{H}$  NMR (300 MHz,  $\text{CDCl}_3$ ):  $\delta$  3.2–3.6 (br m), 2.1–2.5 (br m), 1.0–1.2 (br m). UV/vis ( $\text{CH}_3\text{CN}$ )  $\lambda_{\text{max}}$ , nm: 201, 246, 300, 359, 534.

**$[\text{Fe}(\text{bpyPMOX}_2)_3]^{2+}$ , **7**.** Iron-centered PMOX samples were prepared as described above for  $[\text{Fe}(\text{bpyPEOX}_2)_3]^{2+}$ , typically with halide exchange to the iodide and the following modifications. A representative example of reagent loadings is as follows: **1a** (34.7 mg; 0.0314 mmol), NaI (113 mg; 0.754 mmol),  $\text{CH}_3\text{CN}$  (6.5 mL), MeOX, (849 mg; 9.77 mmol), and dipropylamine (76.2 mg; 0.754 mmol). Following termination, the reaction mixture was concentrated to a red solid. The crude product was purified by dissolving the solid in  $\text{CH}_2\text{Cl}_2$  (5 mL), filtering the solution through Celite, followed by addition of the  $\text{CH}_2\text{Cl}_2$  solution ( $\sim 5$  mL) to  $\text{Et}_2\text{O}$  (30 mL) to produce a red glassy polymer. Yield: 1.60 g; 97%.  $^1\text{H}$  NMR (300 MHz,  $\text{CDCl}_3$ ):  $\delta$  3.2–3.6 (br m), 1.9–2.3 (br m). UV/vis ( $\text{CH}_3\text{CN}$ )  $\lambda_{\text{max}}$ , nm: 205, 299, 360, 533.

**$[\text{Fe}(\text{bpyPPOX}_2)_3]^{2+}$ , **8**.** Iron-centered PPOX samples were prepared as described for  $[\text{Fe}(\text{bpyPEOX}_2)_3]^{2+}$ , typically with halide exchange to the iodide and the following modifications. A representative example of reagent loadings and reaction conditions is as follows: **1a** (4.7 mg; 4.2  $\mu\text{mol}$ ), NaI (15.3 mg; 0.102 mmol),  $\text{CH}_3\text{CN}$  (0.80 mL), and PhOX, (415 mg; 2.82 mmol) were stirred at 100 °C for 1 d and terminated as above with dipropylamine (150 mg; 1.5 mmol). The reaction mixture was concentrated to a red crude solid, which was purified by dissolving the solid in  $\text{CH}_2\text{Cl}_2$  (10 mL) and washing the solution with water ( $3 \times 10$  mL), followed by concentration of the organic layer in vacuo. The solid was redissolved in  $\text{CH}_2\text{Cl}_2$  (5 mL) and precipitated in  $\text{Et}_2\text{O}$  (30 mL) to yield a flocculent red product. Yield: 0.181 g; 48%.  $^1\text{H}$  NMR (300 MHz,  $\text{CD}_2\text{Cl}_2$ ):  $\delta$  7.0–7.5 (br m), 2.8 (br m). UV/vis ( $\text{CH}_3\text{CN}$ )  $\lambda_{\text{max}}$ , nm: 195, 300, 356, 536.

**$[\text{Fe}(\text{bpyPUOX}_2)_3]^{2+}$ , **9**.** Iron-centered PUOX samples were prepared as described above for  $[\text{Fe}(\text{bpyPEOX}_2)_3]^{2+}$  with the following exceptions. A representative example is as follows: **1a** (12.0 mg, 0.0109 mmol),  $\text{CH}_3\text{CN}$  (1.5 mL), PhCl (1.5 mL), and UnOX, (959 mg; 4.26 mmol) were stirred at 110 °C for 15 h and terminated as above with dipropylamine (26.5 mg; 0.262 mmol). The crude product was redissolved in dichloromethane

(3 mL) and was delivered to stirring  $\text{CH}_3\text{CN}$  (35 mL) to precipitate a red crystalline polymer. Yield: 0.580 g; 60%.  $^1\text{H}$  NMR (300 MHz,  $\text{CDCl}_3$ ):  $\delta$  3.2–3.6 (br m), 2.1–2.5 (br m) 1.4–1.7 (br m), 1.0–1.4 (br m), 0.9 (t,  $J = 7$  Hz). UV/vis ( $\text{CHCl}_3$ )  $\lambda_{\text{max}}$ , nm: 240, 290, 360, 536.

**Preparation of bpyPROX<sub>2</sub> Macroligands by Fe Star Fragmentation (R = E, Ethyl; M, Methyl; U, Undecyl; P, Phenyl), 10–13.** The ethyl and undecyl metal-centered polymers were fragmented using previously reported methods.<sup>20</sup> Analogous to the ethyl-substituted polymer, bpyPPOX<sub>2</sub> is prepared in essentially quantitative yield. Metal-free bpyPMOX<sub>2</sub> was prepared as described for bpyPEOX<sub>2</sub> with the following changes in the workup. After stirring for 1 d under air in  $\text{K}_2\text{CO}_3(\text{aq})/\text{CH}_3\text{CN}$ , the mixture was concentrated in vacuo. A heterogeneous mixture of brown and colorless solids resulted. The crude product was dissolved in  $\text{CH}_2\text{Cl}_2$ , filtered through Celite, and concentrated in vacuo to afford a colorless solid. Typical yields: ~90%.  $^1\text{H}$  NMR spectra are indistinguishable from those of the respective Fe-centered polymers. BpyPEOX<sub>2</sub>, **10**, UV/vis ( $\text{CH}_3\text{CN}$ )  $\lambda_{\text{max}}$ , nm: 203, 249, 282. BpyPMOX<sub>2</sub>, **11**, UV/vis ( $\text{CH}_3\text{CN}$ )  $\lambda_{\text{max}}$ , nm: 203, 249 (sh), 283. BpyPPOX<sub>2</sub>, **12**, UV/vis ( $\text{CH}_3\text{CN}$ )  $\lambda_{\text{max}}$ , nm: 198, 238 (sh). BpyPUOX<sub>2</sub>, **13**, UV/vis ( $\text{CHCl}_3$ )  $\lambda_{\text{max}}$ , nm: 241, 250 (sh), 285.

**Polymerization of EtOX with bpy( $\text{CH}_2\text{Cl}$ )<sub>2</sub>.** The initiator bpy( $\text{CH}_2\text{Cl}$ )<sub>2</sub> (20.0 mg; 0.079 mmol),  $\text{CH}_3\text{CN}$  (3.3 mL), and EtOX (1.57 g; 15.8 mmol) were combined in a Kontes flask. The reaction mixture was sealed under  $\text{N}_2$  and stirred at 85 °C for 1 d and then was concentrated in vacuo. (Note: Certain reactions were terminated by stirring with  $\text{HNPr}_2$  for 1 d at 25 °C prior to concentration and molecular weight analysis by GPC.) The crude product was dissolved in  $\text{CH}_2\text{Cl}_2$  and precipitated from  $\text{Et}_2\text{O}$  to afford a yellow solid. Yield: 0.341 g, 22%. Calculated molecular weight based on 100% monomer conversion: 20 100. GPC molecular weight:  $M_n = 13\ 100$ ,  $M_w = 13\ 400$ , PDI = 1.02. The  $^1\text{H}$  NMR spectrum is indistinguishable from that of  $[\text{Fe}(\text{bpyPEOX}_2)_3]^{2+}$ , **6**. UV/vis ( $\text{CH}_3\text{CN}$ )  $\lambda_{\text{max}}$ , nm: 204, 248, 285.

**Polymerization of EtOX with bpy( $\text{CH}_2\text{Cl}$ )<sub>2</sub> and NaI.** The initiator bpy( $\text{CH}_2\text{Cl}$ )<sub>2</sub> (21.0 mg; 0.0829 mmol), NaI (99 mg; 0.66 mmol),  $\text{CH}_3\text{CN}$  (3.3 mL), and EtOX (1.65 g; 16.6 mmol) were combined in a Kontes flask. The reaction mixture was sealed under  $\text{N}_2$  and stirred at 0 °C for 2 h for in situ halide exchange. The mixture was heated at 85 °C for 1 d and then was concentrated in vacuo. The crude product was dissolved in  $\text{CH}_2\text{Cl}_2$  (15 mL) and washed with water (3 × 10 mL). The organic solution was concentrated, and the resulting yellow residue was dissolved in  $\text{CH}_2\text{Cl}_2$  and precipitated from  $\text{Et}_2\text{O}$  to afford a yellow solid. Yield: 1.64 g; 98%. Calcd molecular weight based on 100% monomer conversion: 20 100. GPC molecular weight:  $M_n = 43\ 900$ ,  $M_w = 48\ 300$ , PDI = 1.10. The  $^1\text{H}$  NMR is indistinguishable from that of **6**,  $[\text{Fe}(\text{bpyPEOX}_2)_3]^{2+}$  UV/vis ( $\text{CH}_3\text{CN}$ )  $\lambda_{\text{max}}$ , nm: 204, 245, 284.

**Preparation of  $[\text{Fe}(\text{bpyPEOX}_2)_3]\text{SO}_4$  by Macroligand Chelation.** The macroligand bpyPEOX<sub>2</sub> ( $M_n = 8300$ ; 260 mg; 0.0312 mmol) and MeOH (5 mL) were combined in a Schlenk flask under  $\text{N}_2$ . A MeOH solution of  $\text{Fe}(\text{NH}_4)_2(\text{SO}_4)_2 \cdot 6\text{H}_2\text{O}$  (6.10 mM, 1.70 mL, 10.4  $\mu\text{mol}$ ) was added, and the colorless reaction mixture immediately became dark red. The mixture was stirred at room temperature for 3 h and was concentrated in vacuo to yield a red solid: 0.263 g; 99%. UV/vis ( $\text{CH}_3\text{CN}$ )  $\lambda_{\text{max}}$ , nm: 296, 363, 535.

**Kinetics Experiments.  $[\text{Fe}(\text{bpyPEOX}_2)_3]^{2+}$ .** To a Kontes flask under  $\text{N}_2$  were added, in the following order,  $[\text{Fe}(\text{bpy}(\text{CH}_2\text{Cl})_2)_3](\text{PF}_6)_2$  (45.8 mg; 0.041 mmol),  $\text{CD}_3\text{CN}$  (8.0 mL), 1,3-dioxane (0.21 mL; 2.60 mmol), and 2-ethyl-2-oxazoline (2.47 g; 24.9 mmol). The mixture was stirred at room temperature for ~5 s, and an aliquot was removed for characterization by  $^1\text{H}$  NMR spectroscopy to determine the initial monomer concentration relative to internal standard. The reaction vessel was sealed and stirred at 85 °C. Aliquots were removed at the designated times.  $^1\text{H}$  NMR spectral analysis was performed on a fraction of the sample in order to determine percent monomer conversion. The remaining portion was delivered to  $\text{K}_2\text{CO}_3$  (0.25 g; 1.8 mmol) in  $\text{H}_2\text{O}$  (0.5 mL), was stirred at 80 °C for 1 d, and then was concentrated in vacuo. The residue

was dissolved in  $\text{CH}_2\text{Cl}_2$ , filtered through Celite, and concentrated in vacuo. The resulting colorless polymer was characterized by GPC.

A kinetics study of  $[\text{Fe}(\text{bpyPEOX}_2)_3]^{2+}$  formation from the iodide initiator was performed as described for the chloride **1a**, with the following exceptions: Sodium iodide (0.147 g; 0.98 mmol) was also added to the reaction mixture. After an aliquot ( $t = 0$ ) was removed, the mixture was cooled to 0 °C in an ice bath and stirred for 2 h. The mixture was then heated to 85 °C and treated as described above.

Kinetics analyses of other PROX polymerizations with **1a** were performed as described above for  $[\text{Fe}(\text{bpyPEOX}_2)_3]^{2+}$ , with the indicated reagent loadings.  $[\text{Fe}(\text{bpyPMOX}_2)_3]^{2+}$ ; **1a** (48.5 mg; 0.044 mmol), NaI (158 mg; 1.05 mmol),  $\text{CD}_3\text{CN}$  (7.5 mL), 1,3-dioxane (0.10 mL; 1.2 mmol), and 2-methyl-2-oxazoline (2.24 g; 26.3 mmol), temperature = 85 °C.  $[\text{Fe}(\text{bpyPPOX}_2)_3]^{2+}$ ; **1a** (78.5 mg; 0.071 mmol), NaI (255 mg; 1.70 mmol),  $\text{CD}_3\text{CN}$  (12.0 mL), 1,3-dioxane (0.36 mL; 4.3 mmol), and 2-phenyl-2-oxazoline (6.27 g; 42.6 mmol), temperature = 100 °C.  $[\text{Fe}(\text{bpyPUOX}_2)_3]^{2+}$ ; **1a** (18.7 mg; 0.017 mmol),  $\text{CD}_3\text{CN}$  (1.2 mL),  $\text{C}_6\text{D}_5\text{Cl}$  (1.3 mL), 1,3-dioxane (0.10 mL; 1.2 mmol), and 2-undecyl-2-oxazoline (2.00 g; 8.87 mmol), temperature = 110 °C.

**Thermochromism Studies. (a) Film Preparation.** A hollow Teflon cylinder was clamped to a 25 mm diameter quartz plate forming a cylindrical well (interior diameter = 18 mm) with Teflon walls and a quartz bottom. A solution of  $[\text{Fe}(\text{bpyPEOX}_2)_3]^{2+}$  (25 mg) in  $\text{CH}_3\text{CN}$  (2 mL) was delivered to the well and a film was prepared by slow evaporation under  $\text{N}_2$ . The Teflon cylinder was removed and the resulting film was covered with a second quartz plate.

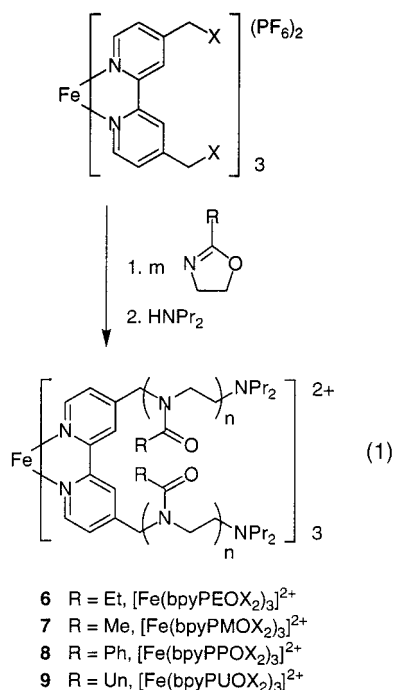
**(b) UV/Vis Spectroscopic Analysis.** The spectrometer was oriented perpendicular to its normal configuration in order to minimize the flow of polymer between the two plates with increased temperature. The hot stage was clamped in place such that the light path ran perpendicular to the film and the ground. The sample cell was continuously purged with  $\text{N}_2$  as it was heated at a rate of 5 °C/min to 210 °C and then cooled to room temperature and cycled once more to 210 °C. During these cycles, spectra were collected at the designated temperatures.

## Results and Discussion

Numerous monodisperse polyoxazolines of different architectures and compositions have been prepared by a living mechanism from electrophilic initiators and 2-R-2-oxazoline monomers (R = alkyl, aryl).<sup>26,34–39</sup> Polymeric metal complexes may be generated in an analogous manner using metal complexes as initiators.<sup>18–21</sup> Success with this divergent metaloinitiator route to polymeric metal complexes requires that the metal complex and its associated counterions not interfere with polymerization, which for polyoxazolines involves electrophilic initiating and propagating species. Herein the iron reagents  $[\text{Fe}\{\text{bpy}(\text{CH}_2\text{X})_2\}_3](\text{PF}_6)_2$ , (**1a**, X = Cl; **1b**, X = I) were explored as initiators for the polymerization of 2-R-2-oxazolines, **2–5**. In another approach, involving synthesis of macroligands followed by their chelation to metal ions, the controlled polymerization must tolerate Lewis basic ligand functionality. To further probe the viability of the macroligand approach, for EtOX, **2**, polymerizations using the ligand initiator, 4,4'-bis-(chloromethyl)-2,2'-bipyridine and the corresponding iodide generated from NaI in situ were also performed. Reactions with EtOX, MeOX, PhOX, and UnOX monomers are described in turn.

**Reactions of Iron Initiators with 2-Ethyl-2-Oxazoline.** Red-violet  $[\text{Fe}(\text{bpyPEOX}_2)_3]^{2+}$  products were prepared by reaction of  $[\text{Fe}\{\text{bpy}(\text{CH}_2\text{Cl})_2\}_3](\text{PF}_6)_2$  with EtOX, **2**, in  $\text{CH}_3\text{CN}$  for 1 d at 85 °C, followed by termination with  $\text{HNPr}_2$  (eq 1). Similar Fe PEOX products were generated from the iodide initiator **1b**,





formed in situ from the chloride **1a**, using NaI.<sup>38</sup> Monomer concentration was typically maintained between 1 and 5 M, depending on the monomer loading per halide initiator site. Iron-centered PEOX stars, **6**, were purified by precipitation from  $\text{CH}_2\text{Cl}_2/\text{Et}_2\text{O}$ . For reactions involving NaI, an aqueous wash was included prior to precipitation to ensure that residual salts were removed. The resulting product,  $[\text{Fe}(\text{bpyPEOX}_2)_3]^{2+}$ , **6**, is soluble in polar solvents such as water, acetonitrile, DMF, and alcohols, as well as in chlorinated solvents such as  $\text{CH}_2\text{Cl}_2$  and  $\text{CHCl}_3$ .

As has been previously observed for PEOX materials, labile metal  $\text{bpyPROX}_2$  complexes fragment when subjected to gel permeation chromatography (GPC).<sup>19,20</sup> This is true regardless of polymer molecular weight and side chain R. The eluting polymer fractions contain little to no evidence of the red violet Fe tris(bpy) chromophores as monitored by in-line diode array UV/vis detection. This observation suggests some fascinating possibilities for use of polymeric metal complexes as materials that respond to mechanical perturbations with associated spectroscopic changes in the visible region. However, partial or complete fragmentation of iron-centered polymers precluded obtaining star molecular weights directly by GPC. Thus,  $\text{bpyPROX}_2$  macroligands (Figure 3) were intentionally liberated from the Fe centers by reaction with  $\text{K}_2\text{CO}_3$  prior to GPC analysis. Cleavage after termination with dipropylamine produces aminotelechelic polymers, whereas direct fragmentation of living polymers with aqueous base is reported to form hydroxytelechelic polymers.<sup>40</sup> This approach provides information about the efficiency of initiation from the halomethyl sites of **1a** and **1b** and about the uniformity of the  $\text{bpyPROX}_2$  macroligands of which the Fe stars are comprised.

It should be noted that cleavage of labile core stars also creates another avenue for metal-centered star-shaped polymer synthesis, namely by metal template-assisted self-assembly. Macroligands can be combined with metal salts to generate a wide variety of new metal-centered polymers.<sup>41</sup> For example, coordination to Fe(II) by  $\text{bpyPEOX}_2$  ( $M_n = 8300$ ) was accomplished

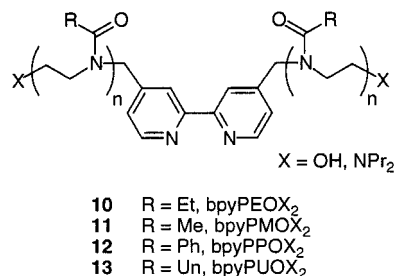


**Figure 3.** Telechelic bipyridine-centered polyoxazoline macroligands.

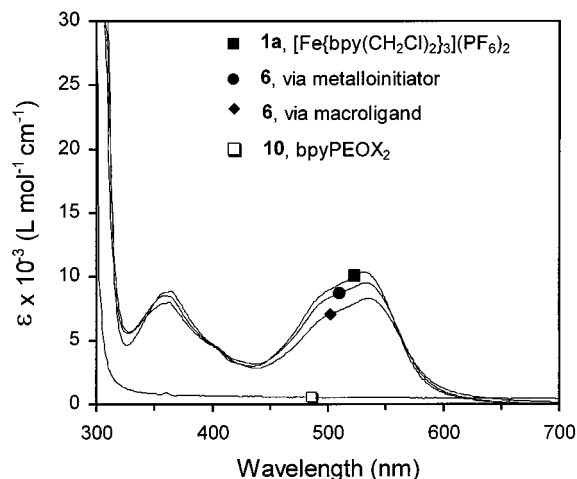


**Figure 4.** Comparison of the UV/vis spectra corresponding to the metal initiator,  $[\text{Fe}\{\text{bpy}(\text{CH}_2\text{Cl})_2\}_3](\text{PF}_6)_2$ , **1a**, the iron-centered polymers,  $[\text{Fe}(\text{bpyPEOX}_2)_3]^{2+}$ , **6**, prepared by the metal initiator and macroligand strategies, and the bipyridine-centered macroligand,  $\text{bpyPEOX}_2$ , **10** (solvent =  $\text{CH}_3\text{CN}$ ).

by reaction with  $\text{Fe}(\text{NH}_4)_2(\text{SO}_4)_2 \cdot 6\text{H}_2\text{O}$  in MeOH. The colorless macroligand solution turned deep red immediately upon delivery of the metal salt, although the reaction was typically stirred for 3 h before isolation and characterization. UV/vis spectra are comparable for the Fe tris(bpy) initiator and for polymeric metal complexes, **6**, prepared in different ways (for MLCT, 532 nm; Fe initiator **1a**,  $\epsilon = 10\,400\text{ M}^{-1}\text{ cm}^{-1}$ ; metal initiator approach,  $\epsilon = 9500\text{ M}^{-1}\text{ cm}^{-1}$ ; macroligand method,  $\epsilon = 8200\text{ M}^{-1}\text{ cm}^{-1}$ ) (Figure 4). This implies that the Fe initiator chromophores survive polymerization in the divergent approach and that reconstitution is reasonably efficient for convergent synthesis by chelation. The  $\text{bpyPROX}_2$  macroligands have also been coordinated to Ru, Cu, and other metals.<sup>42</sup>

Representative molecular weight data obtained for  $\text{bpyPEOX}_2$  macroligands **10**, liberated from the respective  $[\text{Fe}(\text{bpyPEOX}_2)_3]^{2+}$  iron-centered stars, are listed in Table 1 (entries 1–5), along with data for other  $\text{bpyPROX}_2$  materials, **11–13**, prepared in a similar way. Of all the monomers, reactions with EtOX were most controlled. Polymers obtained from preparative reactions with both chloride and iodide initiators generally possess quite narrow molecular weight distributions. It should be noted, however, that PDIs as high as 1.20 measured for certain  $\text{bpyPEOX}_2$  samples (i.e., a difunctional initiator after cleavage) (Table 1) signal either slow initiation relative to propagation or the occurrence of some chain transfer or termination. Molecular weights correlate directly with the expected values based on reaction stoichiometry up to  $M_n^{\text{star}} \approx 75\,000$ , degree of polymerization (DP)  $\approx 750$  (Figure 5). It is possible to

**Table 1. Representative GPC Molecular Weight Data for bpyPROX<sub>2</sub> Macroligands, 10–13, Liberated from [Fe(bpyPROX<sub>2</sub>)<sub>3</sub>]<sup>2+</sup> Stars, 6–9**

entry	monomer	initiator <sup>a</sup>	[M] <sub>0</sub> /[X] <sub>0</sub> <sup>b</sup>	<i>M<sub>n</sub></i> (calcd) <sup>c</sup> (× 10 <sup>3</sup> )	<i>M<sub>n</sub></i> <sup>d</sup> (× 10 <sup>3</sup> )	<i>M<sub>w</sub></i> <sup>d</sup> (× 10 <sup>3</sup> )	PDI <sup>d</sup>
1	EtOX	<b>1a</b>	25	5.0	4.3	5.2	1.20
2	EtOX	<b>1a</b>	50	9.9	10.9	12.0	1.09
3	EtOX	<b>1b</b>	75	14.9	15.3	16.6	1.09
4	EtOX	<b>1a</b>	100	19.8	19.5	20.0	1.03
5	EtOX	<b>1b</b>	125	24.8	25.0	27.0	1.08
6	MeOX	<b>1b</b>	50	8.5	3.9 <sup>e</sup>	6.8 <sup>e</sup>	1.72 <sup>e</sup>
7	MeOX	<b>1a</b>	100	17.0	13.4 <sup>e</sup>	18.1 <sup>e</sup>	1.35 <sup>e</sup>
8	MeOX	<b>1b</b>	130	22.1	17.5 <sup>e</sup>	18.9 <sup>e</sup>	1.08 <sup>e</sup>
9	UnOX	<b>1a</b>	17	7.7	6.4	8.6	1.35
10	UnOX	<b>1a</b>	24	10.8	8.7	11.6	1.34
11	UnOX	<b>1a</b>	33	14.9	11.7	14.0	1.20
12	UnOX	<b>1b</b>	67	30.2	31.5	40.5	1.29
13	UnOX	<b>1a</b>	84	37.9	30.8	35.7	1.16
14	PhOX	<b>1b</b>	30	8.8	11.0	11.7	1.07
15	PhOX	<b>1b</b>	50	14.7	10.8	11.5	1.07
16	PhOX	<b>1b</b>	100	29.4	20.5	21.4	1.05

<sup>a</sup> Key: **1a**, X = Cl; **1b**, X = I. <sup>b</sup> Monomer loading per halide initiator site, X. <sup>c</sup> *M<sub>n</sub>*(calcd) per bpyPROX<sub>2</sub> for 100% monomer conversion. Note: *M<sub>n</sub>*<sup>star</sup> ≈ 3 × bpyPROX<sub>2</sub>. <sup>d</sup> Determined by GPC with MALLS and RI detection in CHCl<sub>3</sub>. <sup>e</sup> Determined vs PMMA standards in DMF containing 0.4% Et<sub>3</sub>N.

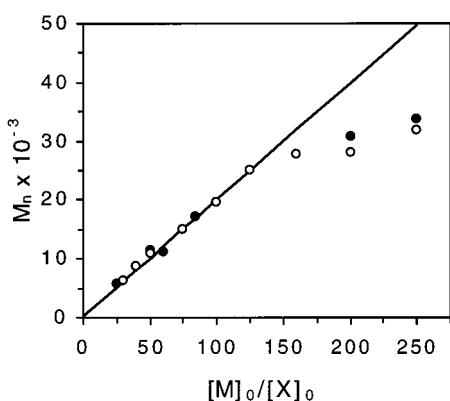


**Figure 5.** Dependence of bpyPEOX<sub>2</sub> number-average molecular weight on monomer loading per halide initiator site, X (solid line, *M<sub>n</sub>*(calcd); closed circles, chloride initiator **1a**; open circles, iodide initiator **1b**). Temperature = 85 °C; solvent = CH<sub>3</sub>CN.

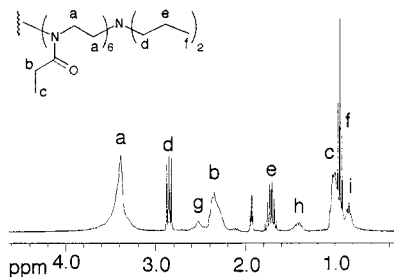


**Figure 6.** <sup>1</sup>H NMR end group analysis of dipropylamine terminated [Fe(bpyPEOX<sub>2</sub>)<sub>3</sub>]<sup>2+</sup>, **6**, in CD<sub>3</sub>CN. (Peaks g–i correspond to unreacted terminating agent, HNPr<sub>2</sub>.)

achieve higher molecular weights up to ~100 000; however, PDIs begin to broaden significantly above this point. Other indications that reactions of EtOX with iron initiators are controlled include the successful preparation of block copolymers<sup>20</sup> and functionalization of the polymer chain ends.

Investigation of low molecular weight [Fe(bpyPEOX<sub>2</sub>)<sub>3</sub>]<sup>2+</sup> ([EtOX]<sub>0</sub>/[**1a**]<sub>0</sub> = 36) by <sup>1</sup>H NMR spectroscopy in CD<sub>3</sub>CN confirms termination of the living polymer by dipropylamine (Figure 6). Integration of the ethylene polymer backbone protons (peak a) vs the methylene protons α to the nitrogen of the terminating group (peak d) reveal a 5.5:1 ratio. This corresponds closely to the

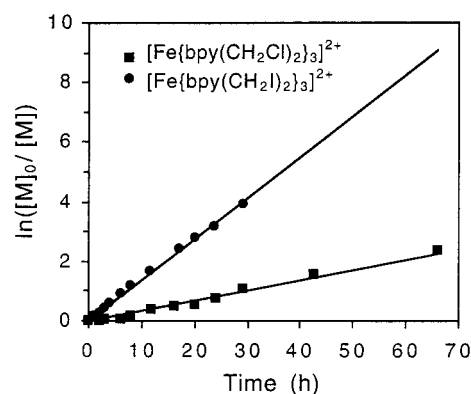


**Figure 7.** First-order kinetics plots for the polymerization of EtOX, **2**, with iron initiators **1a** and **1b**. ([**1a**]<sub>0</sub> = [**1b**]<sub>0</sub> = 3.8 mM; [**2**]<sub>0</sub> = 2.3 M; temperature = 85 °C; solvent = CD<sub>3</sub>CN; rate constants: **1a**: 2.51 × 10<sup>−3</sup> L mol<sup>−1</sup> s<sup>−1</sup>; **1b**: 9.98 × 10<sup>−3</sup> L mol<sup>−1</sup> s<sup>−1</sup>).

6:1 ratio expected for efficient termination of a low molecular weight polymer formed from a 6:1 EtOX/**1a** loading. The chemical shifts corresponding to −N(CH<sub>2</sub>CH<sub>2</sub>CH<sub>3</sub>)<sub>2</sub> end groups (peaks d–f) are slightly downfield from analogous resonances in dipropylamine (peaks g–i).

To further explore the molecular weight control that is achievable in EtOX polymerizations with the Fe initiators **1a** and **1b**, kinetics experiments were performed. Polymerizations were carried out in CD<sub>3</sub>CN, and monomer conversion was determined by <sup>1</sup>H NMR spectroscopy using 1,3-dioxane as an internal standard.<sup>43</sup> As expected, faster reaction rates are observed for the iodide initiator, **1b** as compared to the chloride **1a**. This is illustrated in Figure 7 for EtOX polymerizations, wherein first-order kinetics plots are compared. Rate constants for the Cl and I reactions are 2.51 × 10<sup>−3</sup> and 9.98 × 10<sup>−3</sup> L mol<sup>−1</sup> s<sup>−1</sup>, respectively. Slow initiation, perhaps even an induction period of ~5 h, was observed in the polymerization of EtOX with the chloride initiator **1a**. A linear first-order kinetics plot (Figure 8) is consistent with a controlled polymerization for the chloride initiator and suggests that termination is minimal. The *M<sub>n</sub>* vs percent conversion plot agrees reasonably well with the calculated values; however, the slight curvature that is evident, first decreasing in slope and then increasing at high conversion, could be indica-

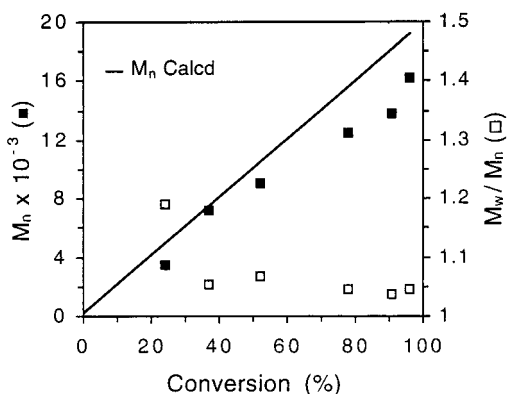


**Figure 8.** Number-average molecular weight vs percent monomer conversion plot for the polymerization of EtOX, **2**, with the metalloinitiator  $[\text{Fe}\{\text{bpy}(\text{CH}_2\text{Cl})_2\}_3](\text{PF}_6)_2$ , **1a** ( $[\mathbf{1a}]_0 = 3.8 \text{ mM}$ ;  $[\mathbf{2}]_0 = 2.3 \text{ M}$ ; temperature =  $85^\circ\text{C}$ ; solvent =  $\text{CD}_3\text{CN}$ ).

tive of some chain transfer and repolymerization, respectively. Linear plots are also observed for the iodide initiator; however, molecular weights obtained in these analytical experiments are lower than expected based on monomer to initiator loading.<sup>44</sup>

**Reactions of Bipyridine Initiators with 2-Ethyl-2-Oxazoline.** As was the case for reactions with Fe initiators, attempts to grow poly(2-ethyl-2-oxazoline) macroligands from 4,4'-bis(halomethyl)-2,2'-bipyridines,  $\text{bpy}(\text{CH}_2\text{X})_2$ , produced polymers with narrow molecular weight distributions. After reaction in  $\text{CH}_3\text{CN}$  at  $80^\circ\text{C}$  for 1 d, nearly quantitative yields were obtained for reactions with the 4,4'-bis(chloromethyl)-2,2'-bipyridine/NaI initiator system, whereas low yields ( $\sim 22\%$ ) were observed when using  $\text{bpy}(\text{CH}_2\text{Cl})_2$  as the initiator. In both cases, however, molecular weights of the resulting polymers were typically higher than anticipated based on monomer conversion (e.g., for the iodide,  $M_n(\text{calcd}) = 20\,100$ ,  $M_n = 43\,900$ ). These differences in reactivity parallel that of benzyl chloride, a poor initiator for EtOX under the aforementioned conditions, and benzyl chloride/NaI, which is a good initiating system (e.g., for  $[\text{EtOX}]_0: [\text{BnCl}]_0 = 100:1$ ,  $M_n(\text{calcd}) = 10\,000$ ,  $M_n = 1000$ ;  $[\text{EtOX}]_0: [\text{BnCl}]_0: [\text{NaI}]_0 = 100:1:4$ ,  $M_n(\text{calcd}) = 10\,000$ ;  $M_n = 9600$ . Reaction conditions:  $\text{CH}_3\text{CN}$ , 1 d,  $80^\circ\text{C}$ ).<sup>18–20,36</sup> In situ halide exchange with metal iodides, NaI or KI,<sup>38</sup> is commonly utilized to activate benzyl chlorides,<sup>36,37,39</sup> if reactions are to be performed at moderate temperatures.

Unlike benzyl chloride, the bipyridine initiators possess nucleophilic nitrogen centers that could compete with EtOX monomer and halide,  $\text{X}^-$ , for reaction with electrophiles at different stages of the polymerization. That is, bpy nitrogens could combine with the initiating sites through self-reaction, or they could attack the growing chain ends, either causing termination or effecting chain transfer (Figure 9). If bpy does not compete well with monomer under the reaction conditions, it is also possible that after all or most monomer is depleted, the bipyridine moieties on one chain could end cap another. Previously, we have noted that 4,4'-bis(bromomethyl)-2,2'-bipyridine and other bpy bromides self-react to form colored pyridinium species both during long-term storage in the freezer, and when  $\text{CDCl}_3$  solutions of the compounds stand at room-temperature overnight. Trace amounts of pyridinium products are also evident in certain preparations of the less reactive analogue,  $\text{bpy}(\text{CH}_2\text{Cl})_2$ . (This compound is

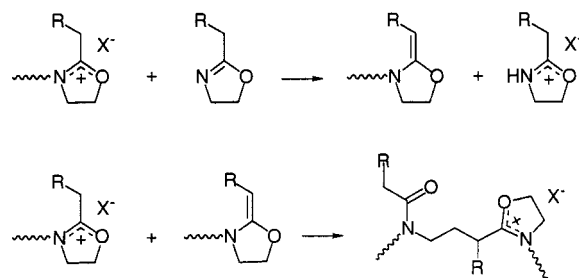


**Figure 9.** Proposed mechanisms for chain transfer to monomer (top) and repolymerization (bottom).<sup>47</sup>

formed through reaction of  $\text{bpy}\{\text{CH}_2\text{Si}(\text{CH}_3)_3\}_2$  with  $\text{Cl}_3\text{-CCl}_3$  in  $\text{CH}_3\text{CN}$  at  $60^\circ\text{C}$  for 4 h,<sup>31</sup> conditions similar to those used for polymerizations.) On the basis of these observations, it seems quite plausible that some initiator molecules, particularly the more reactive iodides, could self-react either during halide exchange with NaI at  $0^\circ\text{C}$  or once the reactions are heated to  $80^\circ\text{C}$  for polymerization. Quantitative initiator dimerization to produce more electrophilic pyridinium species prior to controlled polymerization, could account for the narrow PDIs and higher molecular weights that are observed for the iodide initiator. (e.g., for NaI addition,  $[\text{EtOX}]_0/[\text{bpy}(\text{CH}_2\text{X})_2]_0 = 200$ ;  $M_n(\text{calcd})$  for  $\text{bpy}(\text{CH}_2\text{X})_2$  as initiator = 20 100;  $M_n(\text{calcd})$  for dimer as initiator = 40 000;  $M_n = 43\,900$ ).

In effort to distinguish possible roles for bpy nitrogens and to determine which of the aforementioned side reactions might be occurring, polymerizations with both the iodide and chloride initiating systems were carried out in  $\text{CD}_3\text{CN}$  at a loading of  $[\text{EtOX}]_0/[\text{X}]_0 = 20$  ( $\text{X} =$  initiator halide) and reactions were monitored by  $^1\text{H}$  NMR spectroscopy. After stirring  $\text{bpy}(\text{CH}_2\text{Cl})_2$  with NaI in the presence of EtOX at  $0^\circ\text{C}$  for 2 h, the typical procedure for benzyl halide exchange,<sup>39</sup> it was noted that only a fraction of the initiator ( $\sim 20\%$ ) had converted from the chloride ( $\text{bpy}(\text{CH}_2\text{Cl})_2$ , 4.75 ppm) to the iodide ( $(\text{bpy}(\text{CH}_2\text{I})_2$ , 4.55 ppm). A third bipyridine species ( $\sim 20\%$  of sample), which does not correspond to  $\text{bpyPEOX}_2$ , was also present after halide exchange. (In  $\text{CD}_3\text{CN}$ ,  $^1\text{H}$  NMR:  $\text{bpy}(\text{CH}_2\text{Cl})_2$   $\delta$  8.66, 8.45, 7.44;  $\text{bpy}(\text{CH}_2\text{I})_2$   $\delta$  8.57, 8.41, 7.40; bpy byproduct  $\delta$  7.91, 7.69, 6.95.) It seems unlikely that this byproduct is a pyridinium compound, as bpy resonances typically shift to higher, not lower ppm for the cationic species. Likewise, upon alkylation, the benzylic protons,  $\text{bpyCH}_2\text{N}^+$ , typically appear in the 5–6 ppm region; however, these resonances are not observed. Thus, it is concluded that the amount of pyridinium species arising from initiator self-reaction is negligible at this stage, and even after heating at  $80^\circ\text{C}$  for 30 min. Similarly, no initiator dimerization was observed during polymerization reactions with the less reactive  $\text{bpy}(\text{CH}_2\text{Cl})_2$  run in the absence of NaI. These observations made at the early stages of the reactions rule out quantitative initiator dimerization as a likely explanation for the higher than targeted molecular weights. For the iodide, however, destruction of a portion of the initiator could be a contributing factor.

When reactions of  $\text{bpy}(\text{CH}_2\text{Cl})_2$  with EtOX were conducted without NaI, very poor initiation was observed; even after heating at  $80^\circ\text{C}$  for  $> 1$  day, considerable amounts of unreacted initiator were present. Monomer conversion and polymer molecular weights remain low, and  $^1\text{H}$  NMR spectra show little to no evidence of chain termination by bipyridine attack on



growing chain ends. For the iodide initiating system, in contrast, only trace amounts of unreacted initiators, in chloride or iodide form, were evident in the reaction mixture after 30 min at 80 °C. As the reaction progressed, spectra became complex. Both mono- and difunctional polymers,  $\text{bpy}(\text{CH}_2\text{X})(\text{PEOX})$  and  $\text{bpy-PEOX}_2$ , with trace amounts of self-reacted initiator and the aforementioned bpy byproduct could be present. Whereas reactions with chloride initiators typically proceed by a covalent mechanism for 2-substituted-2-oxazolines, those with added NaI often involve ionic propagating species.<sup>39,45</sup> Resonances at 4.8–4.9 ppm in reactions with  $\text{bpy}(\text{CH}_2\text{Cl})_2/\text{NaI}$  are consistent with those previously assigned to the cationic oxazolinium moiety.<sup>34,39</sup>

Though initiator self-reaction is not a significant factor in reactions with ligand initiators, unprotected bpy nucleophiles might interfere with other stages of the polymerizations. Initially, it was postulated by us<sup>19</sup> and others<sup>23</sup> that bipyridine nitrogens might react with polymer chain ends either to prematurely terminate growing chains, or to end cap fully polymerized living polyoxazolines. Nuyken has noted that end capping reactions between pyridine and living polyoxazolines, forming triflate and tosylate pyridinium salts, occur very slowly at room temperature.<sup>46</sup> Reaction of bpy nucleophiles with electrophilic polymer chain ends should be most favorable once the monomer, a competing nucleophile, is depleted (and before the stronger nucleophile,  $\text{HNPr}_2$  is added to terminate the polymerization). To determine whether this was the case, a comparison was made between reactions with the  $\text{bpy}(\text{CH}_2\text{Cl})_2/\text{NaI}$  initiating system that were terminated after 1 d and those that were run to partial monomer conversion. If chain coupling is more prevalent at the end of the reaction, polymer molecular weights are expected to rise relative to targeted values for reactions that are run to completion, as compared with those that are terminated early. A comparison of measured degrees of polymerization at partial conversion (~67%) with those once most monomer had been consumed (~98%) for the iodide initiator and an initial monomer loading of  $[\text{EtOX}]/[\text{X}] = 100$  indicated that termination of the chain ends by bipyridine could be occurring to some extent: 67% conversion,  $\text{DP}_{\text{expt}}/\text{DP}_{\text{calcd}} = 1.58$ ; 98% conversion,  $\text{DP}_{\text{expt}}/\text{DP}_{\text{calcd}} = 2.24$ . It should be noted, however, that the anticipated changes in chemical shifts and peak intensities that are expected if the postulated pyridinium species is formed were not detected by  $^1\text{H}$  NMR.

For  $^1\text{H}$  NMR scale reactions with the  $\text{bpy}(\text{CH}_2\text{Cl})_2$  initiator run at low monomer loading, significant quantities of new species with resonances consistent with pyridinium compounds (i.e., 5.3–6.3 ppm “benzylic” and downfield bpy resonances) were observed in spectra when the “living” polymer was concentrated in vacuo prior to end-capping the electrophilic chain ends with dipropylamine. The fact that “pyridinium” resonances disappear after purification of polymer samples by precipitation suggests that these particular resonances do not arise from termination or end capping of the polymer chain. Instead, unreacted  $\text{bpy}(\text{CH}_2\text{Cl})_2$  initiator may dimerize upon concentration and perhaps remain in the  $\text{CH}_2\text{Cl}_2/\text{Et}_2\text{O}$  filtrate fraction upon polymer precipitation. However, the fact that GPC molecular weights are somewhat elevated for unterminated reactions indicates that chain coupling cannot be ruled out

(unterminated polymer:  $M_n = 13\,100$ ,  $\text{PDI} = 1.02$ , reaction time = 1 d;  $\text{HNPr}_2$  terminated polymer  $M_n = 7900$ ,  $\text{PDI} = 1.06$ , reaction time = ~2 d).

Another important factor to take into account in evaluating reactions with  $\text{bpy}(\text{CH}_2\text{X})_2$  initiators is the effect that these reagents might have upon chain transfer. One proposed mechanism for this side reaction involves chain transfer to monomer (Figure 9).<sup>47</sup> In this case, monomer functions first as a base to deprotonate the oxazolinium species, thus forming both an unsaturated chain end that is believed to participate in repolymerization and an activated monomer that may function as a new kind of initiator. Like the monomer, bipyridine could also function as a base to deprotonate the growing chain end; however, unlike the monomer, the resulting protonated bpy is not expected to function as a polymerization initiator. With both chloride and iodide ligand initiating systems, GPC traces ( $\text{CHCl}_3$ ) reveal some tailing on the lower molecular weight side of the main polymer fractions as well as significant high molecular weight shoulders, signatures of chain transfer and repolymerization. These features are considerably more pronounced than what is seen for certain reactions with Fe initiators **1a** and **1b**. It must be noted, however, that termination by bpy could give rise to similar features in GPC traces, thus making it difficult to distinguish these two effects in this manner.

In summary, for  $\text{bpy}(\text{CH}_2\text{Cl})_2$ , poor initiator efficiency combined with bipyridine termination and chain transfer (i.e., repolymerization) are all factors that could account for the high molecular weights that are observed in EtOX reactions. For the iodide, initiation is far more efficient; although if the observed byproduct is not a competent initiator, diminished quantities of initiator would also lead to increased molecular weights. It is puzzling that PDIs remain narrow in these reactions, despite the fact that initiation is slow for the chloride and certain side reactions are occurring. Samples were analyzed in  $\text{CHCl}_3$  for ready comparison with literature precedent. However, it has been previously noted by us for Ru systems,<sup>21</sup> and by others,<sup>39</sup> that, in some cases, polyoxazolines can present difficulties for molecular weight characterization due to interaction with GPC columns. Though less extreme for metal-free  $\text{bpyPEOX}_2$  macroligands than for metal-containing stars,<sup>21</sup> this could account for the narrow PDIs that are observed.

**Implications of Findings with Ligand Initiators for the Role of Iron in Polymerizations with Metalloinitiators.** A comparison of results obtained for Fe initiators **1a** and **1b** with those for  $\text{bpy}(\text{CH}_2\text{X})_2$  initiators suggests that the Fe(II) ions play an important role in EtOX polymerizations. Coordination to metals serves to protect the bpy nitrogens, thus shutting down termination and preventing bpy from functioning as a base in chain transfer reactions. Moreover, because Fe(II) is a Lewis acid, the initiator sites in  $[\text{Fe}\{\text{bpy}(\text{CH}_2\text{X})_2\}](\text{PF}_6)_2$  are more electrophilic and reactive, compared to the uncoordinated ligands. The fact that yields and monomer conversion are so low for reactions initiated by  $\text{bpy}(\text{CH}_2\text{Cl})_2$  relative to the corresponding iron complex **1a**, even after very long reaction times, suggests that some feature of the metalloinitiator may also be serving as an activator not just for initiation but also for propagation. Further evidence that this is the case was seen in control reactions with benzyl chloride run in the presence and absence of  $[\text{Fe}(\text{bpy})_3](\text{PF}_6)_2$ . In

this case, there are no Lewis basic sites for Fe to bind and activate the initiator. Nonetheless, a pronounced effect upon monomer conversion is observed (compare EtOX/BnCl = 100/1,  $M_n$  = 1500, PDI = 1.35 and EtOX/BnCl/Fe = 600/6/1,  $M_n$  = 12,500, PDI = 1.10). For the more reactive iodide, in contrast, no significant differences were observed between reactions with and without Fe present (EtOX/BnCl/NaI = 100/1/1,  $M_n$  = 13 100, PDI = 1.04; EtOX/BnCl/NaI/Fe = 600/6/24/1,  $M_n$  = 13 900, PDI = 1.02).<sup>48</sup> Others have noted that  $\text{PF}_6^-$  and other fluoride-containing counterions can serve to terminate cationic oxazoline polymerizations.<sup>49</sup> However, this does not seem to be a major factor in reactions with Fe initiators **1a** and **1b** nor in those with benzyl halide initiators. No diminution of control is observed in reactions with Fe present relative to those without—PDIs remain narrow and molecular weights are comparable. Other control reactions likewise show no major role for  $\text{PF}_6^-$  salts in these reactions.<sup>21</sup> It has been proposed by others that coordination of monomer to metals could be responsible for the activation.<sup>50</sup> Though Fe(II) is coordinatively saturated in the tris(bpy) complex, it is labile and could readily dissociate a ligand, to open up a coordination site. However, since chelation to metal ions would decrease monomer nucleophilicity, Fe is not likely to enhance attack on the reactive chain end in this way. Another possibility is that interaction of Lewis acids with monomer could cause it to function as an initiator.<sup>51</sup> But since molecular weights of polymerizations with Fe initiators are close to targeted values, this does not seem to be occurring. Iron(II) association with the chain end might make it more electrophilic and susceptible to a nucleophilic attack, but this seems most likely after ring opening, since repulsion between Fe and chain end cations would be expected beforehand with the oxazolinium species. In conclusion, the manner in which iron tris(bpy) with its associated  $\text{PF}_6^-$  counterions serves to activate EtOX polymerization is not yet understood.

**Reactions of Iron Initiators with Other 2-R-2-Oxazolines (R = Methyl, Phenyl, Undecyl).** Polymerizations of other monomers with Fe initiators were less controlled than EtOX. Reactions of MeOX with iron initiators were performed as described for EtOX. Red-violet  $[\text{Fe}(\text{bpyPMOX}_2)_3]^{2+}$  and the corresponding colorless macroligand formed emulsions that did not clarify during aqueous workup. Thus, excess NaI was removed by filtration of  $\text{CH}_2\text{Cl}_2$  solutions through Celite. Because chloroform is a poor solvent for GPC of PMOX samples, molecular weight analysis was performed with DMF containing 0.4%  $\text{Et}_3\text{N}$  as the mobile phase. Often poorer correlation between targeted and experimental molecular weights and broader PDIs were observed for bpyPMOX<sub>2</sub> samples as compared with bpyPEOX<sub>2</sub> (Figure 10, Table 1). This could be due, in part, to the fact that molecular weights are determined vs PMMA standards, which may not be a good comparison for bpyPMOX<sub>2</sub>. However, there is also evidence of chain transfer in GPC traces, particularly at longer reaction times. The fact that first-order kinetics plots are linear for MeOX reactions initiated by **1b** (Figure 11) suggests that termination is negligible and that the number and reactivity of active species remain constant, which is consistent with the proposed mechanism for chain transfer in oxazoline polymerizations (Figure 9).<sup>47</sup>

The phenyl-substituted oxazoline, **4**, is the least reactive of the four monomers that were explored. A

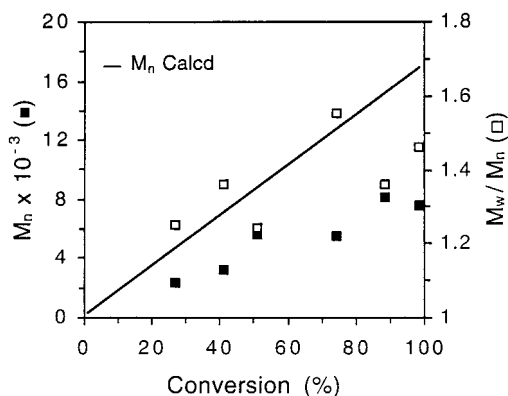


**Figure 10.** Number-average molecular weight vs percent monomer conversion plot for the polymerization of MeOX, **3**, with the metalloinitiator  $[\text{Fe}(\text{bpy}(\text{CH}_2\text{I})_2)_3](\text{PF}_6)_2$ , **1b** ( $[\text{1b}]_0$  = 8.6 mM;  $[\text{3}]_0$  = 5.1 M; temperature = 85 °C; solvent =  $\text{CD}_3\text{CN}$ ).

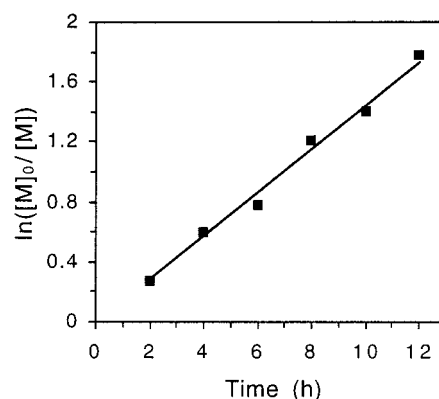


**Figure 11.** First-order kinetics plot for the polymerization of MeOX, **3**, using  $[\text{Fe}(\text{bpy}(\text{CH}_2\text{I})_2)_3](\text{PF}_6)_2$ , **1b** ( $[\text{1b}]_0$  = 8.6 mM;  $[\text{3}]_0$  = 5.1 M; temperature = 85 °C; solvent =  $\text{CD}_3\text{CN}$ ;  $k$  =  $4.65 \times 10^{-3} \text{ L mol}^{-1} \text{ s}^{-1}$ ).

**Table 2. Molecular Weight Data for bpyPPOX<sub>2</sub>, **12**, Liberated from  $[\text{Fe}(\text{bpyPPOX}_2)_3]^{2+}$  Polymers, **8**, Prepared under Different Reaction Conditions<sup>a</sup>**

entry	initiator <sup>b</sup>	temp (°C)	solvent(s)	$M_n^d$ ( $\times 10^3$ )	$M_w^d$ ( $\times 10^3$ )	PDI <sup>d</sup>	yield (%) <sup>e</sup>
1	<b>1a</b>	80	$\text{CH}_3\text{CN}$	2.6	2.8	1.08	6
2	<b>1b</b>	80	$\text{CH}_3\text{CN}$	10.0	11.4	1.14	48
3	<b>1a</b>	100	$\text{CH}_3\text{CN}$	12.7	14.3	1.13	35
4	<b>1b</b>	100	$\text{CH}_3\text{CN}$	20.5	21.4	1.04	57
5	<b>1a</b>	80	$\text{CH}_3\text{CN}/\text{PhCl}^c$	4.6	6.5	1.41	10
6	<b>1a</b>	100	$\text{CH}_3\text{CN}/\text{PhCl}^c$	15.6	18.0	1.15	38

<sup>a</sup> Key:  $[\text{1}]_0$  = 3.7 mM;  $[\text{4}]_0$  = 2.2 M; PhOX:Fe = 600:1;  $M_n(\text{calcd})$  = 29 800; reaction time = 1 d; terminated with dipropylamine, 25 °C, 1 d. <sup>b</sup> Key: **1a**, X = Cl; **1b**, X = I. <sup>c</sup>  $\text{CH}_3\text{CN}$ : PhCl = 3:1 v/v. <sup>d</sup> Per bpyPPOX<sub>2</sub>; molecular weights (MALLS and RI detection in  $\text{CHCl}_3$ ) for bpyPPOX<sub>2</sub> obtained after treatment of Fe stars with aqueous  $\text{K}_2\text{CO}_3$ . Star  $M_n \approx 3 \times M_n$  bpyPPOX<sub>2</sub>. <sup>e</sup> Yields are based on mass recovery after precipitation from  $\text{CH}_2\text{Cl}_2/\text{Et}_2\text{O}$ , relative to initial monomer loading.

variety of different reaction conditions were investigated in an attempt to increase molecular weights and yields of  $[\text{Fe}(\text{bpyPPOX}_2)_3]^{2+}$ , **8**. Representative results of varying the solvent, the halide initiating system, and the temperature for reactions with **4** are given in Table 2. Maximum yields and molecular weights and the lowest polydispersities were obtained for reactions run with the iodide initiating system in acetonitrile solution at 100 °C (see entry 4). Hence, these conditions were used for preparative and kinetics runs. Similar to the Fe-centered PEOX and PMOX materials,  $[\text{Fe}(\text{bpyPPOX}_2)_3]^{2+}$ ,



**Table 3. Representative Molecular Weight Data for bpyPUOX<sub>2</sub>, 13, Liberated from [Fe(bpyPUOX<sub>2</sub>)<sub>3</sub>]<sup>2+</sup> Polymers, 9, That Were Prepared under Different Reaction Conditions**

entry	initiator <sup>a</sup>	temp (°C)	solvent(s)	$M_n(\text{calcd})^b (\times 10^3)$	$M_n^c (\times 10^3)$	$M_w^c (\times 10^3)$	PDI <sup>c</sup>	yield (%)
1 <sup>d</sup>	<b>1b</b>	100	CH <sub>3</sub> CN	9.5	2.2	5.1	2.30	30
2 <sup>e</sup>	<b>1a</b>	100	ODCB	30.2	31.5	40.5	1.29	<sup>g</sup>
3 <sup>f</sup>	<b>1a</b>	110	CH <sub>3</sub> CN/PhCl	37.9	30.8	35.7	1.16	90

<sup>a</sup> Key: **1a**, X = Cl; **1b**, X = I. <sup>b</sup>  $M_n(\text{calcd})$  per bpyPUOX<sub>2</sub> for 100% monomer conversion. Star  $M_n \approx 3 \times \text{bpyPUOX}_2 M_n$ . <sup>c</sup> Determined by GPC with MALLS and RI detection. <sup>d</sup>  $[\mathbf{1b}]_0 = 4.1 \text{ mM}$ ;  $[\mathbf{5}]_0 = 0.5 \text{ M}$ ; 127 equiv of UnOX per initiator; reaction time = 15 h. <sup>e</sup>  $[\mathbf{1a}]_0 = 6.9 \text{ mM}$ ;  $[\mathbf{5}]_0 = 2.8 \text{ M}$ ; 403 equiv of UnOX per initiator; reaction time = 8 h. <sup>f</sup>  $[\mathbf{1a}]_0 = 3.8 \text{ mM}$ ;  $[\mathbf{5}]_0 = 2.0 \text{ M}$ ; 504 equiv of UnOX per initiator; reaction time = 8 h; CH<sub>3</sub>CN: PhCl = 1:1, vol:vol. <sup>g</sup> Aliquot removed for characterization of the first block in diblock copolymer synthesis.

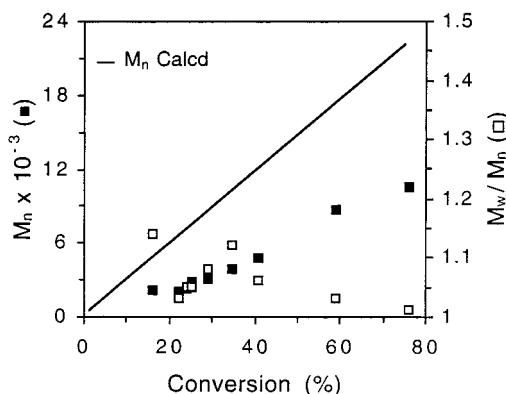


**Figure 12.** Number-average molecular weight vs percent monomer conversion plot for the polymerization of PhOX, **4**, with  $[\text{Fe}\{\text{bpy}(\text{CH}_2\text{I})_2\}_3](\text{PF}_6)_2$ , **1b**, as the initiator ( $[\mathbf{1b}]_0 = 4.5 \text{ mM}$ ;  $[\mathbf{4}]_0 = 2.7 \text{ M}$ ; temperature = 100 °C; solvent = CD<sub>3</sub>CN).

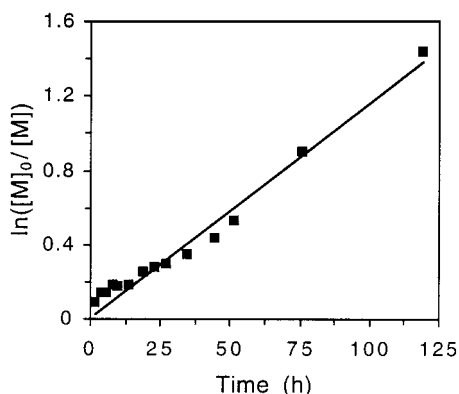


**Figure 13.** First-order kinetics plot for the polymerization of PhOX, **4**, using  $[\text{Fe}\{\text{bpy}(\text{CH}_2\text{I})_2\}_3](\text{PF}_6)_2$ , **1b** ( $[\mathbf{1b}]_0 = 4.5 \text{ mM}$ ;  $[\mathbf{4}]_0 = 2.7 \text{ M}$ ; temperature = 100 °C; solvent = CD<sub>3</sub>CN;  $k = 8.18 \times 10^{-4} \text{ L mol}^{-1} \text{ s}^{-1}$ ).

**8**, is a red-violet glassy polymer that is soluble in CH<sub>3</sub>CN, CH<sub>2</sub>Cl<sub>2</sub>, and CHCl<sub>3</sub>. It is conveniently purified by precipitation from CH<sub>2</sub>Cl<sub>2</sub>/Et<sub>2</sub>O. As for PMOX, PPOX samples show poor correlation between experimental molecular weights and those anticipated based on monomer loading (Figure 12). Also typical for nonliving reactions, first-order kinetics plots are nonlinear (Figure 13). PDIs remain narrow throughout, but increase slightly with monomer conversion up to ~35% conversion (~1.5 d), at which point PDIs drop and the kinetics plot shows indication of changes in the rate of monomer consumption. Others have noted that GPC of PPOX materials can be quite sensitive to workup and thermal conditioning prior to analysis.<sup>35</sup> However, no sign of interaction with GPC columns was noted in this case. Typically, neither high molecular weight shoulders nor tailing associated with chain transfer are evident in GPC traces of PPOX samples. In summary, though reactions of initiators **1a** and **1b** with PhOX are not living, narrow polydispersity iron-containing materials

are obtained with molecular weights that are, to some extent, controllable by reaction stoichiometry. Block copolymers have also been prepared.<sup>20</sup>

Attempts to polymerize UnOX, **5**, by the conditions employed for EtOX and MeOX generated materials with very poor molecular weight control (e.g., Table 3, entry 1). After several hours, the growing polymer precipitated from CH<sub>3</sub>CN solution, and over time (~15 h) the reaction became highly viscous such that stirring ceased. A low molecular weight polymer with a broad molecular weight distribution was obtained. For a better match with the less polar UnOX monomer and resulting  $[\text{Fe}(\text{bpyPUOX}_2)_3]^{2+}$  polymer, *o*-dichlorobenzene<sup>35</sup> (ODCB) and an elevated reaction temperature were applied (Table 3, entry 2). This resulted in higher molecular weight polymer with a lower polydispersity index. Ultimately, chlorobenzene<sup>39</sup> (PhCl) was substituted for ODCB in these reactions because similar molecular weight control was observed and it was much easier to remove residual amounts of lower boiling PhCl. However, since the dicationic Fe initiator is not entirely soluble in either ODCB or PhCl, a CH<sub>3</sub>CN/PhCl mixed solvent system was employed. After screening different CH<sub>3</sub>CN/PhCl ratios, it was discovered that a 1:1 (vol: vol) mixture was optimal both for fully dissolving the initiator **1a** at the onset and for ensuring that the polymer product remained in solution at the end of the reaction once most of the monomer was consumed. This adjustment resulted in a slightly lower PDI and molecular weights close to the targeted values. In contrast to the other iron-centered polyoxazolines, **6–8**, which are glassy,  $[\text{Fe}(\text{bpyPUOX}_2)_3]^{2+}$ , **9**, is a crystalline polymer that is soluble in CH<sub>2</sub>Cl<sub>2</sub> and CHCl<sub>3</sub> but is insoluble in diethyl ether, as well as in polar solvents such as DMF, CH<sub>3</sub>CN, alcohols, and water. The undecyl polymer, **9**, was purified by precipitation from CH<sub>2</sub>Cl<sub>2</sub>/CH<sub>3</sub>CN or alternatively, by trituration with Et<sub>2</sub>O to remove residual PhCl and unreacted monomer.

Addition of NaI to polymerizations of UnOX in CD<sub>3</sub>CN/C<sub>6</sub>D<sub>5</sub>Cl in attempt to form **1b** in situ resulted in essentially no rate acceleration, perhaps due to poor halide exchange in this less polar reaction mixture. However, polymerizations of UnOX with the chloride **1a** show a linear relationship between  $M_n$  and percent monomer conversion (Figure 14) and good correlation between experimental molecular weights and those calculated based upon reaction stoichiometry (Table 1). A nonlinear relationship between  $\ln([\text{monomer}]_0/[\text{monomer}])$  and time was observed for reactions of UnOX with **1a** (Figure 15), which is perhaps indicative of slow initiation and rate acceleration as the reaction progresses. Riffle et al.<sup>39</sup> have reported similar behavior for the polymerization of EtOX by benzyl iodide in chlorobenzene. They noted that propagation was faster at the later stages of the reaction when an ionic oxazolinium mechanism predominated, as compared to initiation and the early stages of the reaction when covalent species

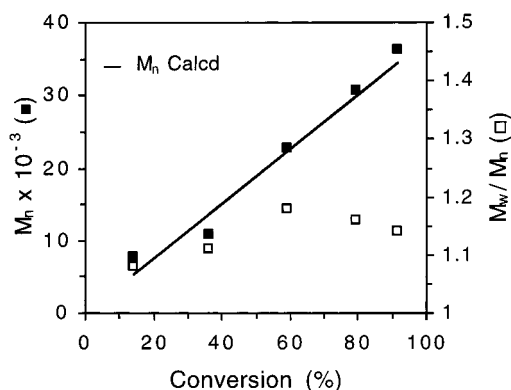


**Figure 14.** Number-average molecular weight vs percent monomer conversion plot for the polymerization of UnOX, **5**, with the metalloinitiator  $[\text{Fe}\{\text{bpy}(\text{CH}_2\text{Cl})_2\}_3](\text{PF}_6)_2$ , **1a** ( $[\mathbf{1a}]_0 = 3.8 \text{ mM}$ ;  $[\mathbf{5}]_0 = 2.0 \text{ M}$ ; temperature =  $110^\circ\text{C}$ ; solvent =  $\text{CD}_3\text{CN}/\text{C}_6\text{D}_5\text{Cl}$ ).

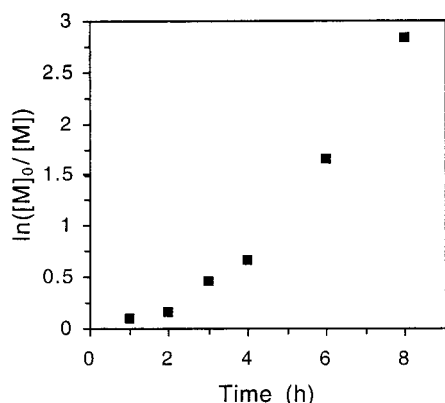


**Figure 15.** Kinetics plot for the polymerization of UnOX, **5**, with  $[\text{Fe}\{\text{bpy}(\text{CH}_2\text{Cl})_2\}_3](\text{PF}_6)_2$ , **1a** ( $[\mathbf{1a}]_0 = 3.8 \text{ mM}$ ;  $[\mathbf{5}]_0 = 2.0 \text{ M}$ ; temperature =  $110^\circ\text{C}$ ; solvent =  $\text{CD}_3\text{CN}/\text{C}_6\text{D}_5\text{Cl}$ ).

**Table 4. DSC Analysis of  $[\text{Fe}(\text{bpyPROX}_2)_3]^{2+}$  Stars, **6–9**, and  $\text{bpyPROX}_2$  Macroligands, **10–13**<sup>a</sup>**

sample	$M_n$ ( $\times 10^{-3}$ )	$T_g$ ( $^\circ\text{C}$ ) <sup>b</sup>	$T_m$ ( $^\circ\text{C}$ ) <sup>c</sup>	$\Delta H_m$ (J/g)	$\Delta S_m^d$ (J/g $^\circ\text{C}$ )
$[\text{Fe}(\text{bpyPEOX}_2)_3]^{2+}$	55.2	55			
$\text{bpyPEOX}_2$	18.6	55			
$[\text{Fe}(\text{bpyPMOX}_2)_3]^{2+}$	40.2	46			
$\text{bpyPMOX}_2$	13.4	45			
$[\text{Fe}(\text{bpyPUOX}_2)_3]^{2+}$	48.6		132, 141	32	0.23
$\text{bpyPUOX}_2$	16.2		132, 142	32	0.23
$[\text{Fe}(\text{bpyPPOX}_2)_3]^{2+}$	33.0	103	159, 185 <sup>e</sup>	18	0.097
$\text{bpyPPOX}_2$	11.0	99	149, 205 <sup>e</sup>	30	0.15

<sup>a</sup> All thermal events were measured during the second heating cycle. <sup>b</sup> Middle of the change in the heat capacity. <sup>c</sup> Onset, peak. <sup>d</sup> Calculated from  $\Delta S_m = \Delta H_m/T_m$ . <sup>e</sup> Measured from the first heating cycle.

were evident. This can lead to broadening of the PDIs even though  $M_n$  vs conversion plots are linear.

**Thermal Analysis of BpyPROX<sub>2</sub> and Fe PROX Materials.** The thermal properties of  $[\text{Fe}(\text{bpyPROX}_2)_3]^{2+}$  polymers were monitored by modulated differential scanning calorimetry (MDSC), thermogravimetric analysis (TGA) and by variable-temperature UV/vis spectral analysis. DSC data for the metal-containing polymers and the metal-free macroligands are listed in Table 4. Only a minor variation was displayed between the thermal events of the metal and metal-free polymers (molecular weight range: 11 000–55 200). The methyl-, ethyl-, and phenyl-substituted Fe-centered star-shaped polymers exhibited glass transitions at 45, 55, and 103

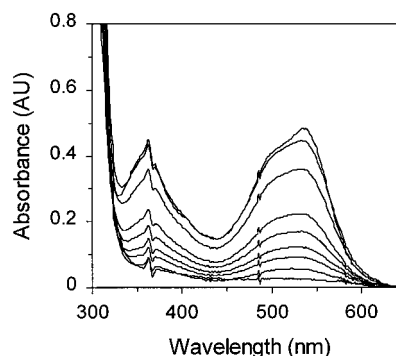


**Figure 16.** Thermochromic behavior of  $[\text{Fe}(\text{bpyPEOX}_2)_3]^{2+}$ , **6**, illustrated by variable UV/vis spectroscopy ( $M_n = 18\,000$ ; temperature ( $^\circ\text{C}$ ) = 25, 85, 100, 115, 130, 150, 165, 180, and 210, for descending absorbances at  $\lambda_{\text{max}} = 535 \text{ nm}$ ).

$^\circ\text{C}$ , respectively. The crystalline undecyl polymers,  $[\text{Fe}(\text{bpyPUOX}_2)_3]^{2+}$  displayed a melt with an onset point of  $132^\circ\text{C}$  and a  $\Delta H_m = 32 \text{ J/g}$ . The changes in entropy upon melting,  $\Delta S_m$ , were calculated as  $0.23 \text{ J/g } ^\circ\text{C}$  for each. A crystallization was observed in the cooling cycle for both the Fe-centered star ( $99^\circ\text{C}$ ;  $\Delta H_{\text{crys}} = -37 \text{ J/g}$ ) and linear ( $101^\circ\text{C}$ ;  $\Delta H_{\text{crys}} = -36 \text{ J/g}$ ) PUOX samples. These observations are consistent with previous findings of analogous metal-free polyoxazolines.<sup>35,52,53</sup>

In addition to a glass transition, the phenyl-substituted polymer showed a very broad endotherm with a maximum signal for the star-shaped and linear samples at 185 and  $205^\circ\text{C}$ , respectively. Thermodynamic data for this transition revealed a marked difference between the star ( $\Delta H_m = 18 \text{ J/g}$ ) and the more crystalline linear sample ( $\Delta H_m = 30 \text{ J/g}$ ). This transition was only evident in the first heating cycle and could be due to residual crystallization. These events are close to, but lower than, melting temperatures observed for PPOX materials in the  $210\text{--}237^\circ\text{C}$  range in previous studies.<sup>52</sup>

Thermogravimetric analysis under nitrogen revealed the undecyl analogue to be the most robust of the Fe-centered polymers. The PUOX sample ( $M_n = 48\,600$ ) showed 5% weight loss at  $360^\circ\text{C}$  and underwent rapid decomposition at an onset of  $397^\circ\text{C}$ . The ethyl-substituted polymer ( $M_n = 55\,200$ ) showed 5% weight loss at  $334^\circ\text{C}$  and onset of further decomposition at  $387^\circ\text{C}$ . The  $[\text{Fe}(\text{bpyPMOX}_2)_3]^{2+}$  ( $M_n = 40\,200$ ) and  $[\text{Fe}(\text{bpyPPOX}_2)_3]^{2+}$  ( $M_n = 33\,000$ ) had 5% weight loss at  $227$  and  $339^\circ\text{C}$ , respectively, and both exhibited onset of further decomposition at  $370^\circ\text{C}$ . The hygroscopic PEOX and PMOX Fe-centered polymers lost mass at lower temperatures perhaps due to evaporation of water.

Previously we have noted that Fe tris(bpy)-centered polyoxazolines exhibit reversible thermochromism when samples are heated under a nitrogen atmosphere.<sup>19</sup> DSC thermal analysis revealed no differences between Fe PROX samples and metal-free macroligands, not even in the range where the red-violet polymers begin to fade ( $\sim 100\text{--}180^\circ\text{C}$ ). Variable temperature UV/vis data illustrating the bleaching of the metal to ligand charge transfer (MLCT) band at  $\sim 535 \text{ nm}$  of an Fe-centered PEOX film heated under nitrogen are provided in Figure 16. Cooling and reheating a second time revealed that this process is at least partially reversible for all  $[\text{Fe}(\text{bpyPROX}_2)_3]^{2+}$  samples, **6–9**. Increased sample fluidity correlating with changes in sample thickness as the films are heated complicated quantitative analysis of this effect by the described methods. Hydrophobic

PUOX and PPOX showed the greatest tendency to flow from the quartz cell during heating cycles. A new UV/vis cell must be designed before detailed analysis of the dependence of thermochromism upon polymer molecular weight and side chain will be profitable. Although the exact mechanism of thermochromism of Fe tris(bipyridine) polymer films is not yet known, preliminary observations seem most consistent with reversible ligand dissociation or a thermally induced spin transition, as have been described for many other related iron complexes.<sup>54–57</sup> Detailed magnetic and spectroscopic studies designed to distinguish between these two likely mechanisms will serve as the subject of a future report.

## Conclusion

Functionalized iron tris(bipyridine) reagents are effective initiators for the polymerization of a variety of different oxazoline monomers. The degree of polymerization and level of control that are attainable vary with the monomer, with EtOX showing the greatest versatility. All polymers maintain the red-violet color of the initiator chromophores and exhibit reversible thermochromism, becoming colorless upon heating. The control afforded in the synthesis of these new metal-containing polymers and the interesting thermal, mechanical, and optical phenomenon that they exhibit all indicate that further investigation of physical properties and exploration of possible applications of these materials is merited.

**Acknowledgment.** This work was supported by the National Science Foundation (PECASE Award, CAREER Award and Research Planning Grant), the donors of the Petroleum Research Fund (Type G grant), administered by the American Chemical Society, the Jeffress Foundation, Dupont (Young Professor Grant), and the University of Virginia. We thank GFS Chemicals for additional resources in support of this project. Dr. Jaydeep J. S. Lamba and Benjamin P. Peters are acknowledged for their preliminary contributions to this project.

## References and Notes

- (1) Nguyen, P.; Gómez-Elipé, P.; Mannes, I. *Chem. Rev.* **1999**, *99*, 1515.
- (2) Ciardelli, F.; Tsuchida, E.; Wöhrle, D. *Macromolecule-Metal Complexes*; Springer: Berlin, 1996.
- (3) Kingsborough, R. P.; Swager, T. M. *Prog. Inorg. Chem.* **1999**, *48*, 123.
- (4) Sono, M.; Roach, M. P.; Coulter, E. D.; Dawson, J. H. *Chem. Rev.* **1996**, *96*, 2841.
- (5) Lindley, P. F. *Rep. Prog. Phys.* **1996**, *59*, 867.
- (6) Gray, H. B.; Winkler, J. R. *Annu. Rev. Biochem.* **1996**, *65*, 537.
- (7) Karlin, K. D. *Science* **1993**, *261*, 701.
- (8) Dandliker, P. J.; Diederich, F.; Gisselbrecht, J.-P.; Louati, A.; Gross, M. *Angew. Chem., Int. Ed. Engl.* **1995**, *34*, 2725.
- (9) Jiang, D.-L.; Aida, T. *Chem. Commun.* **1996**, 1523.
- (10) Jiang, D.-L.; Aida, T. *J. Macromol. Sci.—Pure Appl. Chem.* **1997**, *A34*, 2407.
- (11) Castro, R.; Cuadrado, I.; Alonzo, B.; Casado, C. M.; Morán, M.; Kaifer, A. E. *J. Am. Chem. Soc.* **1997**, *119*, 5760.
- (12) Massey, J. A.; Power, K. N.; Winnik, M. A.; Mannes, I. *Adv. Mater.* **1998**, *10*, 1559.
- (13) Peckham, T. J.; Massey, J. A.; Honeyman, C. H.; Mannes, I. *Macromolecules* **1999**, *32*, 2830.
- (14) Newkome, G. R.; He, E.; Moorefield, C. N. *Chem. Rev.* **1999**, *99*, 1689.
- (15) Male, J. L.; Lindfors, B. E.; Covert, K. J.; Tyler, D. R. *Macromolecules* **1997**, *30*, 6404.
- (16) Nieckarz, G. F.; Litty, J. J.; Tyler, D. R. *J. Organomet. Chem.* **1998**, *554*, 19.
- (17) (a) Chujo, Y.; Sada, K.; Saegusa, T. *Macromolecules* **1993**, *26*, 6315. (b) Chujo, Y.; Sada, K.; Saegusa, T. *Macromolecules* **1993**, *26*, 6320.
- (18) Lamba, J. J. S.; McAlvin, J. E.; Peters, B. P.; Fraser, C. L. *Polym. Prepr. (Am. Chem. Soc., Div. Polym. Chem.)* **1997**, *38* (1), 193.
- (19) Lamba, J. J. S.; Fraser, C. L. *J. Am. Chem. Soc.* **1997**, *119*, 1801.
- (20) McAlvin, J. E.; Fraser, C. L. *Macromolecules* **1999**, *32*, 1341.
- (21) McAlvin, J. E.; Fraser, C. L. *Macromolecules* **1999**, *32*, 6295.
- (22) Collins, J. E.; Fraser, C. L. *Macromolecules* **1998**, *31*, 6715.
- (23) Hochwimmer, G.; Nuyken, O.; Schubert, U. S. *Macromol. Rapid Commun.* **1998**, *19*, 309.
- (24) Schubert, U. S.; Nuyken, O.; Hochwimmer, G. *Polym. Mater. Sci. Eng.* **1999**, *80*, 193.
- (25) Schubert, U. S.; Eschbaumer, C.; Hochwimmer, G. *Tetrahedron Lett.* **1998**, *39*, 8643.
- (26) (a) Aoi, K.; Okada, M. *Prog. Polym. Sci.* **1996**, *21*, 151. (b) Chujo, Y.; Saegusa, T. In *Ring Opening Polymerization*; Brunelle, D. J., Ed.; Carl Hanser Verlag: Munich, Germany, 1993; pp 239–262.
- (27) (a) Kwon, I. C.; Bae, Y. H.; Kim, S. W. *Nature* **1991**, *354*, 291. (b) Lee, S. C.; Chang, Y.; Yoon, J.-S.; Kim, C.; Kwon, I. C.; Kim, Y.-H.; Jeong, S. Y. *Macromolecules* **1999**, *32*, 1847.
- (28) Park, C.; Thomas, E. L.; McAlvin, J. E.; Fraser, C. L. Unpublished results.
- (29) Perrin, D. D.; Armarego, W. L. F. *Purification of Laboratory Chemicals*; Third ed.; Butterworth-Heinemann: Oxford, England, 1988.
- (30) Jung, W.; Mayer, C. *Liebigs Ann. Chem.* **1974**, 996.
- (31) Fraser, C. L.; Anastasi, N. R.; Lamba, J. J. S. *J. Org. Chem.* **1997**, *62*, 9314.
- (32) Gould, S.; Strouse, G. F.; Meyer, T. J.; Sullivan, B. P. *Inorg. Chem.* **1991**, *30*, 2942.
- (33) Excess NaI was removed by filtration through Celite. Attempts to further purify PMOX samples by washing CH<sub>2</sub>Cl<sub>2</sub> solutions with H<sub>2</sub>O resulted in inseparable emulsions.
- (34) Saegusa, T.; Kobayashi, S.; Yamada, A. *Makromol. Chem.* **1976**, *177*, 2271.
- (35) Cai, G.; Litt, M. H. *J. Polym. Chem., Part A: Polym. Chem.* **1989**, *27*, 3603.
- (36) Kobayashi, S.; Uyama, H.; Narita, Y. *Macromolecules* **1992**, *25*, 3232.
- (37) For an example of initiation with benzyl chlorides at elevated temperature (benzonitrile/DMF, 150 °C), see: Nuyken, O.; Rueda-Sanchez, J.; Voit, B. *Polym. Bull.* **1997**, *38*, 657.
- (38) Kobayashi, S.; Uyama, H.; Narita, Y. *Macromolecules* **1990**, *23*, 353.
- (39) Liu, Q.; Konas, M.; Riffle, J. S. *Macromolecules* **1993**, *26*, 5572.
- (40) Kobayashi, S.; Masuda, E.; Shoda, S.-I. *Macromolecules* **1989**, *22*, 2878.
- (41) (a) Wu, X.; Fraser, C. L. *Macromolecules* **2000**, *33*, 4053. (b) Wu, X.; Fraser, C. L. In press. (c) Wu, X.; Smith, A. P.; Fraser, C. L. In press.
- (42) McAlvin, J. E.; Fraser, C. L. Unpublished results.
- (43) Control reactions using benzyl chloride as the initiator, both with and without NaI in the presence and absence of 1,3-dioxane, yielded polymers with comparable molecular weight data, confirming that 1,3-dioxane is innocent and suitable for this purpose.
- (44) Preparative reactions with EtOX show better correlation between calculated and measured molecular weights than do analytical scale reactions when NaI is added. Polymerizations may be sensitive to repeated removal of aliquots for <sup>1</sup>H NMR and GPC analysis.
- (45) Saegusa, T.; Ikeda, H. *Macromolecules* **1973**, *6*, 808.
- (46) Nuyken, O.; Maier, G.; Gross, A. *Macromol. Chem. Phys.* **1996**, *197*, 83.
- (47) Litt, M.; Levy, A.; Herz, J. J. *Macromol. Sci., Chem.* **1975**, *A9*, 703.
- (48) Addition of [Fe(bpy)<sub>3</sub>](PF<sub>6</sub>)<sub>2</sub> to EtOX polymerizations with [Ru(bpy)<sub>n</sub>(bpy(CH<sub>2</sub>Cl)<sub>2</sub>)<sub>3–n</sub>](PF<sub>6</sub>)<sub>2</sub> initiators did not serve to activate the polymerizations relative to Fe-free reactions.
- (49) Personal communication, Prof. Morton Litt. Mention has also been made of the use of PhN<sub>2</sub><sup>+</sup>PF<sub>6</sub><sup>–</sup> as an initiator.<sup>47</sup> It was indicated that the reaction gave an 80% overall yield, however the particular monomer and other details of the reaction were not provided.



- (50) Jin, R.-H.; Motoyoshi, K.-I. *J. Porphyrins Phthalocyanines* **1999**, *3*, 60.
- (51) Tomalia, D. A.; Sheetz, D. P. *J. Polym. Sci. Part A-1* **1966**, *4*, 2253.
- (52) Bassiri, T. G.; Levy, A.; Litt, M. *Polym. Lett.* **1967**, *5*, 871.
- (53) Chen, C. H.; Wilson, J.; Chen, W.; Davis, R. M.; Riffle, J. S. *Polymer* **1994**, *35*, 3587.
- (54) Goodwin, H. A. *Coord. Chem. Rev.* **1976**, *18*, 293.
- (55) Gütllich, P.; Jung, J. *J. Mol. Struct.* **1995**, *347*, 21.
- (56) Buchen, T.; Gütllich, P. *Chem. Phys. Lett.* **1994**, *220*, 262.
- (57) König, E.; Ritter, G.; Kulshreshtha, S. K. *Chem. Rev.* **1985**, *85*, 219.

MA000024Q